

## Evaluation Of The Rotor Aerodynamics Of A Wind Turbine Using Combined Blade Element And Momentum Theory

K.R. AJAO

Department of Mechanical Engineering, University of Ilorin, Ilorin, Nigeria

e-mail: [ajaomech@unilorin.edu.ng](mailto:ajaomech@unilorin.edu.ng)

I.K. ADEGUN

Department of Mechanical Engineering, University of Ilorin, Ilorin, Nigeria

e-mail: [kadegun2000@yahoo.com](mailto:kadegun2000@yahoo.com)

**Abstract:** The analysis of the rotor aerodynamics is based on the combined blade element and momentum theory and the content is directed toward the physics of power extraction by wind turbines at both the near and far wake regions. The near wake is the area just behind the rotor, where the properties of the rotor can be discriminated, so approximately up to one rotor diameter downstream and the far wake is the region beyond the near wake, where the focus is put on the influence of the wind turbines in farm situations. A wind turbine extracts energy from the wind by producing a step change in static pressure across the rotor-swept surface. Turbine rotor is the component which exhibits the largest proportion of fatigue failure and the centrifugal and gravity loads are primarily responsible. The generalized Fokker-Planck equation which is a partial differential equation satisfied by the probability density function is employed in modeling the turbine power. [Researcher. 2009;1(3):73-83]. (ISSN: 1553-9865).

**Keywords:** Rotor aerodynamics, near wake, far wake, rotor-swept surface, turbine power.

### 1. Introduction

The conversion of wind energy to useful energy involves two processes: the primary process of extracting kinetic energy from wind and conversion to mechanical energy at the rotor axis, and the secondary process of the conversion into useful energy, mostly electrical energy [1]. Wind turbines extract energy from the wind by producing a step change in static pressure across the rotor-swept surface. As the air approaches the rotor it slows down gradually, resulting in an increase in static pressure. The reduction in static pressure across the rotor disk results in the air behind it being at sub atmospheric pressure. As the air proceeds downstream the pressure climbs back to the atmospheric value resulting in a further slowing down of the wind. There is therefore a reduction in the kinetic energy in the wind, some of which is converted into useful energy by the turbine [2].

The major field science involved in this process is aerodynamics, but it needs meteorology (wind description) as input, and system dynamics for the interaction with the structure. The latter is important since all movement of the rotor blades, including bending of the blades out of their plane of rotation, induces apparent velocities that can influence or even destabilize the energy conversion process. Aerodynamics is the oldest science in wind energy; in 1915, Lanchester [3] was the first to predict the maximum power output of an ideal wind turbine. A major break-through was achieved by Glauert [4], by formulating the blade element momentum (BEM) method. This method extended with many 'engineering rules' is still the basis for all rotor design codes.

Progress is significant in the 30-year history of modern wind energy. Nevertheless, many phenomena are still not fully understood or quantified. This is due to several aspects that are unique for wind turbine aerodynamics.

## 2. Generalized Actuator disc model

To aid the understanding of combined blade element and momentum theory it is useful initially to consider the rotor as an “actuator disc”. Although this model is very simple, it does provide valuable insight into the aerodynamics of the rotor. In fluid mechanics the actuator disc is defined as a discontinuous surface or line on which surface forces act upon the surrounding flow. In rotary aerodynamics the concept of the actuator disc is not new. Indeed, the actuator disc constitutes the main ingredient in the one-dimensional momentum theory, as formulated by Froude [5] and the ‘classical’ BEM method by Glauert. Some of the assumptions made are that, thrust load and velocity are uniform over the disc and the upstream and downstream, the pressure is freestream static pressure.

Usually, the actuator disc is employed in combination with a simplified set of equations and its range of applicability is often confused with the particular set of equations considered.

In the case of a horizontal axis wind turbine the actuator disc is given as a permeable surface normal to the freestream direction on which an evenly distribution of blade forces acts upon the flow. In its general form the flow field is governed by the unsteady, axisymmetric Euler or Navier-stokes equations, which means that no physical restrictions need to be imposed on the kinematics of the flow.

The first Non-linear actuator disc model for heavily loaded propellers was formulated by Wu [6]. Although no actual calculations were carried out, this work demonstrated the opportunities for employing the actuator disc on complicated configurations as e.g. ducted propellers and propellers with finite hubs. Later improvements, especially on the numerical treatment of the equations are due to [7,8] and recently Conway [9,10] has developed further the analytical treatment of the method. In the application of the actuator disc concept for wind turbine aerodynamics the first non-linear model was suggested by Madsen [11], who developed an actuator cylinder model to describe the flow field about a vertical-axis wind turbine, the Gyro mill. This model has later been adapted to treat horizontal axis wind turbines. Recent development of the method has mainly been directed towards the use Navier-stokes equations.

### 2.1 The Navier-Stokes Equations

In a numerical actuator disc model, the Navier-stokes (or Euler) equations are typically solved by a second order accurate finite difference volume scheme as in a usual computational fluid dynamics (CFD) computation. Equations:

$$\frac{\partial \vec{V}^{\rho}}{\partial t} = \nabla \cdot (\vec{V}^{\rho} \otimes \vec{V}^{\rho}) = -\frac{1}{\rho} \nabla P + \nu \nabla^2 \left[ \left( 1 + \frac{\nu_t}{\nu} \right) \nabla \vec{V}^{\rho} \right] + \vec{f}^{\rho} \quad (1)$$

$$\nabla \cdot \vec{V}^{\rho} = 0, \quad (2)$$

Where  $\vec{V}^{\rho}$  denote Reynolds-averaged velocity,  $P$  is the pressure denotes time and  $\rho$  is the density of the fluid and  $\nu$  is the kinematic viscosity. The Reynolds stresses are modeled by the eddy-viscosity,  $\nu_t$  and body force,  $\vec{f}^{\rho}$ , is introduce in order to model external forces fields.

These equations constitute three transport equations, which are parabolic in time and elliptic in space, and equation of continuity stating that the velocity is solenoidal. The main difficulty of this formulation is that the pressure does not appear explicitly in the equation of continuity. The role of the pressure, however, is to ensure the continuity equation be satisfied at every time instant. A way to circumvent this problem is to relate the pressure to the continuity equation by introducing an artificial compressibility term into this [12]. Thus, an artificial transport equation for the pressure is solved along with the three momentum, equations ensuring a solenoidal velocity field when a steady state is achieved. The drawback of this method is that only time-independent problems can be considered.

Another approach, the pressure correction method, is to relate the velocity and pressure fields through the solution of a Poisson equation for the pressure. This is obtained by taking the divergence of the momentum equations, resulting in the following relation:

$$\nabla^2 P = -\rho \nabla \cdot \left[ \nabla \cdot (\vec{V}^{\rho} \otimes \vec{V}^{\rho}) - \nu_t \nabla^2 \vec{V}^{\rho} \right] \quad (3)$$

which is solved iteratively along with the momentum equations. As an alternative to the  $\vec{V} - P$  formulation of the Navier-stokes equations, vorticity based models may be employed. The vorticity, defined as the curl of the time-average velocity

$$\vec{\omega}^* = \nabla \times \vec{V} \tag{4}$$

This is introduced as primary variable by taking the Curl Eqn. (1).The result is the following set of equations:

$$\frac{\partial \vec{\omega}^*}{\partial t} + \nabla \times (\vec{\omega}^* \times \vec{V}) = -\nu \nabla^2 \left[ \left( 1 + \frac{v_t}{\nu} \right) \vec{\omega}^* \right] + \nabla \times \vec{f} + \mathcal{Q}_\omega \tag{5}$$

$$\nabla \times \vec{V} = \vec{\omega}^*, \quad \nabla \cdot \vec{V} = 0, \tag{6}$$

Where  $\mathcal{Q}_\omega$  contains some additional second order terms from the Curl operation. The equations can be formulated in various ways. The Cauchy-Riemann part of Eqn.(6) may be replaced by a set of Poisson equations

$$\nabla^2 \times \vec{V} = -\nabla \times \vec{\omega}^* \tag{7}$$

If we consider Eqn.(5) in an arbitrarily moving frame of reference we get

$$\frac{\partial \vec{\omega}^*}{\partial t} + \nabla \times (\vec{\omega}^* \times \vec{V}) = -\nu \nabla^2 \left[ \left( 1 + \frac{v_t}{\nu} \right) \vec{\omega}^* \right] + \nabla \times \vec{f} + \mathcal{Q}_\omega, \tag{8}$$

Where the velocity vector  $\vec{\omega}^*$  refers to the inertial system

$$\begin{aligned} \vec{\omega}^* &= \vec{\omega} + 2\vec{\Omega} \\ \vec{\Omega} &= (\Omega_x, \Omega_y, \Omega_z) \end{aligned} \tag{9}$$

$\vec{\Omega}$  denotes the angular velocity of the coordinate system. However, the geometry of the blades and the viscous flow around the blades are not resolved. Instead the swept surface of the blades is replaced by surface forces that act upon the incoming flow at a rate corresponding to the period-averaged mechanical work that the rotor extracts from the flow.

In the simple case of an actuator disc with constant prescribed loading, various fundamental studies can be easily carried out. Comparisons with experiments have demonstrated that the method works well for axisymmetric flow conditions and can provide useful information regarding basic assumptions underlying the momentum approach [13,14] turbulent wake states occurring for heavily loaded rotors [15,16], and rotors subject to coning [17,18].

When computing the flow past an actual wind turbine, the aerodynamic forces acting on the rotor are determined from two-dimensional aerofoil characteristic, corrected for three-dimensional effects, using a blade-element approach.

In Figure1, a cross-sectional element at radius  $r_i$  defines the aerofoil in the  $(\theta, z)$  plane.

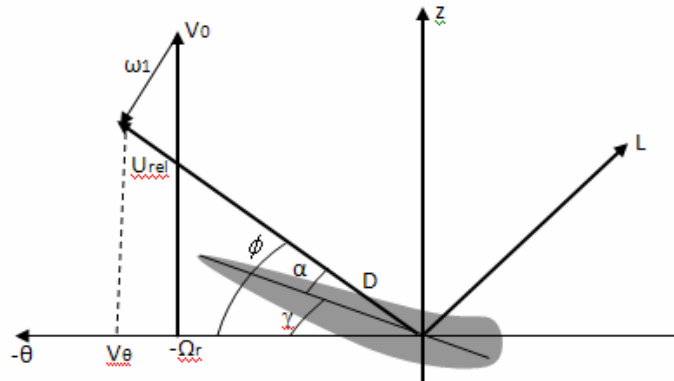


Figure 1. Cross-sectional aerofoil element

Denoting the tangential and axial velocity in the inertia frame of reference as  $V_\theta$  and  $V_z$  respectively. The local velocity relative to the rotating blade is given as

$$V_{rel} = (V_\theta - \Omega r, V_z). \quad (10)$$

The angle of attack is defined as

$$\alpha = \phi - \gamma, \quad (11)$$

Where  $\phi = \tan^{-1} \left( \frac{V_z}{(\Omega r - V_\theta)} \right)$  is the angle between  $V_{rel}$  and the rotor plane.

The distribution of the surface forces, ie force per unit rotor area is given by the following expressions:

$$f_{2D} = \frac{dF}{dA} = \frac{1}{2} \rho V_{rel}^2 Bc (C_L e_L + C_D e_D) / (2\pi r_i) \quad (12)$$

Where  $C_L = C_L(\alpha, R_e)$  and  $C_D = C_D(\alpha, R_e)$  are the lift and drag coefficients respectively is the chord length is the numbers of blades and  $e_L$  and  $e_D$  denote the unit vectors in the directions of the lift and drag respectively.

### 2.11 Lift and Drag Coefficients

The lift and drag coefficients are defined for an aerofoil by

$$C_L = L / \left( \frac{1}{2} \rho V^2 S^* \right) \quad (13)$$

$$C_D = D / \left( \frac{1}{2} \rho V^2 S^* \right) \quad (14)$$

Where L and D are the lift and drag forces,  $S^*$  is the platform area of the aerofoil.

The lift and drag coefficients are determined from measured or computed two-dimensional aerofoil data that are corrected for three-dimensional effects. There are several reasons why it is necessary to correct the aerofoil data. First, at separation rotational effects limit the growth of the boundary layer, resulting in an increased lift as compared to two-dimensional characteristics. Next, the aerofoil characteristics depend on the aspect ratio of the blade. This is in particular pronounced at high incidences where the finite aspect ratio drag coefficient,  $C_D$ , is much smaller than the corresponding one for an infinite blade.

As an example, for a flat plate at an incidence  $\alpha=90^\circ$ , the drag coefficient  $C_D=2$  for an infinitely long plate, whereas for aspect ratio corresponding to the geometry of a wind blade  $C_D$  takes values in the range 1.2-1.3.

Hoerner [19] stated that the normal force from a flat plate is approximately constant for  $45^\circ < \alpha < 135^\circ$ , indicating that in this range both  $C_L$  and  $C_D$  have to be reduced equally.

Hassen [20] proposed to reduce  $C_L$  and  $C_D$  by an expression that takes values in range from 0.6 to 1.0, depending on the ratio between the distance to the tip and the local chord length. It should be noticed, however that this is only a crude guideline and that most aerofoil data for wind turbine use is calibrated against actual performance and load measurement.

### 3. Blade-Element Model

Combined blade element and momentum theory is an extension of the actuator disc theory described above. The rotor blades are divided into a number of blade elements and the theory outlined above used not for the rotor disc as a whole but for a series of annuli swept out by each blade element and where each annulus is assumed to act in the same way as an independent actuator disc. At each radial position the rate of change of axial and angular momentum are equated with the thrust and torque produced by each blade element.

The thrust  $dT$  developed by a blade element of length  $dr'$  located at radius  $r'$  is given by

$$dT = \frac{1}{2} \rho W_i^2 (C_L \cos \phi + C_D \sin \phi) c dr' \quad (15)$$

Where  $W_i$  is the magnitude of the apparent wind speed vector at the blade element.

Also, the torque  $dQ$  developed by the blade element of length  $dr'$  is given by

$$dQ = \frac{1}{2} \rho W^2 r' (C_L \sin \phi - C_D \cos \phi) c dr' \quad (16)$$

In order to solve for the axial and tangential flow induction factors appropriate to the radial position of a particular blade element, the thrust and torque developed by the element are equated to the rate of change of axial and angular momentum similar to those derived for the actuator disc.

The annular induction factors may be expressed as follows

$$a = \frac{g_1}{(1 + g_1)}, a' = \frac{g_2}{(1 - g_2)} \quad (17)$$

$$\text{Where, } g_1 = \frac{Bc}{2\pi r'} \frac{(C_L \cos \phi + C_D \sin \phi)}{4F \sin^2 \phi} H$$

$$\text{And, } g_2 = \frac{Bc}{2\pi r'} \frac{(C_L \sin \phi - C_D \cos \phi)}{4F \sin \phi \cos \phi} \quad (18)$$

The parameter H is defined as follows:

$$\text{for } a \leq 0.3539, H = 1.0, \text{ and for } a > 0.3539, H = \frac{4a(1 - a)}{(0.6 + 0.61a + 0.79a^2)}$$

In the situation where the axial induction factor  $a$  is greater than 0.5, the rotor is heavily loaded and operating in what is referred to as the “turbulent wake state”.

#### 4. Modeling the Wind

The wind field incidence on the turbine may be specified in a number of ways. For some simple calculations, a uniform, constant wind speed is assumed, such that the same incident wind speed is seen by every point on the rotor. For more detailed calculation however, it is important to be able to define both the spatial and temporal variations in wind speed and direction.

The steady-state spatial characteristics of the wind field may include any combination of the following elements, wind shear, tower shadow and upwind turbine wake. When regarding wakes, a distinct division can be made into the near and far wake region. The near wake is taken as the area just behind the rotor, where the properties of the rotor can be discriminated, so approximately up to one rotor diameter downstream. Here, the presence of the rotor is apparent by the number of blades, blade aerodynamics, including stalled flow, 3-D effects and the tip vortices.

The far wake is the region beyond the near wake, where the focus is put on the influence of the wind turbines in farm situations. Here the focus is on wake models, wake interference, turbulence models and topographical effects.

##### 4.1 Near wake Computations

Although there exist a large variety of method for predicting performance and loadings of wind turbines, the most widely used approach today is based on the blade element and momentum theory. A basic assumption in the BEM theory is that the flow takes place in independent stream tubes and that the loading is determined from two-dimensional aerofoil characteristics. The advantage of the model is that it is easy to implement, it contains most of the physics representing rotary aerodynamics, and it has proven to be accurate for the most common flow conditions and rotor configurations. A drawback of the model is that it, to a large extent relies on empirical input which is not always available. Even in the simple case of a rotor subject to steady axial inflow, aerofoil characteristics have to be implemented from wind tunnel measurements. The description is further complicated if we look at more realistic operating situation. Wind turbines are subject to atmospheric turbulence, wind shear from the ground effect, wind directions that change both in time and in space, and effect from the wake of nearby wind turbines.

When the wind changes direction, misalignment with the rotational axis occurs, resulting in yaw error. This causes periodic variation in the angle of attack and invalidates the assumption of axisymmetric inflow conditions. Furthermore, it gives rise to radial flow component in the boundary layer. Thus both the aerofoil characteristics and the wake are subjected to complicated three-dimensional and unsteady flow

behaviour, which only in an approximate way can be implemented in the standard BEM method. In all cases there is a need to develop three-dimensional models from which parametrical studies can be performed.

#### 4.1.1 Vortex Wake Modeling

Vortex wake models denote a class of methods in which the rotor blades and the trailing and shed vortices in the wake are represented by lifting lines or surfaces. At the blades the vortex strength is determined from the bound circulation which is related to the local inflow field. The trailing wake is generated by spanwise variations of the bound vorticity along the blade. The shed wake is generated by the temporal variations as the blade rotate.

Assuming that the flow in the region outside the trailing and shed vortices is curl-free, the overall flow field can be represented by the Biot-Savart law. This is most easily shown by decomposing the velocity in solenoidal part and a rotational part, using Helmholtz decomposition:

$$\vec{V} = \nabla \times \vec{A} + \nabla \Phi \quad (19)$$

Where  $\vec{A}$  is a vector potential and  $\Phi$  a scalar potential.

The vector potential automatically satisfies the continuity Eqn. (2), and from the definition of vorticity, Eqn.(4), we get

$$\nabla^2 \vec{A} = -\vec{\omega} \quad (20)$$

In the absence of boundaries, this can be expressed as an integral relation:

$$\vec{A}(\vec{X}) = \frac{1}{4\pi} \int \frac{\vec{\omega}'}{|\vec{X} - \vec{X}'|} dV_{ol} \quad (21)$$

Where  $\vec{X}$  denotes the point where the potential is computed and the integration is taking over the region where the vorticity is non-zero, designated by  $V_{ol}$ .

From the definition Eqn.(19), the resulting velocity field is obtained by

$$\vec{V}(\vec{X}) = -\frac{1}{4\pi} \int \frac{(\vec{X} - \vec{X}') \times \vec{\omega}'}{|\vec{X} - \vec{X}'|^3} dV_{ol} \quad (22)$$

This is the most usual form of the Biot-Savart law.

In its simplest form the wake is prescribed as hub vortex plus a spiraling tip vortex or as a series of ring vortices. In this case the vortex system is assumed to consist of a number of line vortices with vorticity distribution

$$\omega(\vec{X}) = \Gamma \delta(\vec{X} - \vec{X}') \quad (23)$$

Where  $\Gamma$  is the circulation,  $\delta$  is the Dirac delta function and  $\vec{X}'$  is the curve defining the location of the vortex lines.

Combining this with Eqn.(22) results in

$$\vec{V}(\vec{X}) = -\frac{1}{4\pi} \int_s \Gamma \frac{(\vec{X} - \vec{X}')}{|\vec{X} - \vec{X}'|^3} \times \frac{\partial \vec{X}'}{\partial s'} ds' \quad (24)$$

Where  $s$  is the curve defining the vortex line and  $s'$  is the parametric variable along the curve. Utilizing Eqn.(24), simple vortex models can be derived to compute quite general flow fields about wind turbine rotors.

In a study of Miller [21], a system of vortex rings was used to compute the flow past a heavily loaded wind turbine. It is remarkable to simulate the vortex ring/turbulent wake state with good accuracy, as compared to the empirical correction suggested by Glauert [2].

#### 4.1.2 Far Wake Computations

If the turbine rotor being model led is assumed to be wholly or partially immersed in the wake of another turbine operating further upwind, a model is provided to define the modification to the steady-state mean wind profile caused by that wake.

A Gaussian profile is used to describe the wake of the upstream turbine. The local velocity at a distance  $r$  from the wake centerline (which may be offset from the hub position) is given by:

$$V = V_o \left[ 1 - \Delta e^{-\frac{r^2}{2W^2}} \right] \quad (25)$$

Where  $V_o$  is the undisturbed wind speed,  $\Delta$  is the fractional centerline velocity deficit, and  $W$  is the width of the wake.

To define the velocity deficit  $\Delta$  and the wake width  $W$ , the eddy viscosity model is used.

**[i] Eddy viscosity wake model**

The eddy viscosity wake model is a calculation of the velocity deficit field using a finite-difference solution of the thin shear layer equation of the Navier-Stokes equations in axisymmetric co-ordinates. The eddy viscosity model automatically observes the conservation of mass and momentum in the wake. An eddy viscosity, averaged across each downstream wake section, is used to relate the shear stress term in the thin shear equation to gradients of velocity deficit. The mean field can be obtained by a linear superposition of the wake deficit field and the incident wind flow.

An illustration of the wake profile used in the eddy viscosity model is shown in Figure 2.

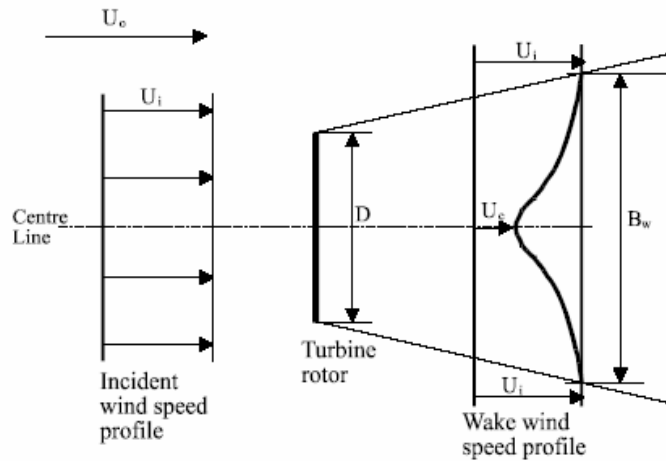


Figure 7.1: Wake profile used in the eddy viscosity model

Figure 2: Wake profile used in eddy viscosity model

The Navier stokes equations with Reynolds stresses and the viscous terms dropped gives:

$$U \frac{\partial U}{\partial x} + V \frac{\partial U}{\partial r} = -\frac{1}{r} \frac{\partial(ruv)}{\partial r} \quad (26)$$

The turbulent viscosity concept is used to describe the shear stresses with an eddy viscosity defined by [22].

$$\varepsilon(x) = L_m(x) \cdot U_m(x)$$

$$\text{and} \quad -uv = \varepsilon \frac{\partial U}{\partial r} \quad (27)$$

$L_m$  and  $U_m$  are suitable length and velocity scales of the turbulence as a function of the downstream distance  $x$  but independent of  $r$ . The length scale is taken as proportional to the wake width  $B_w$  and the velocity scale is proportional to the difference  $U_i - U_c$  across the shear layer.



Thus the shear stress  $\overline{uv}$  is expressed in terms of the eddy viscosity. The governing differential equation to be solved becomes:

$$U \frac{\partial U}{\partial x} + V \frac{\partial U}{\partial r} = \frac{\varepsilon}{r} \frac{\partial(r\partial U / \partial r)}{\partial r} \quad (28)$$

Because of the effect of ambient turbulence, the eddy viscosity in the wake cannot be wholly described by the shear contribution alone. Hence an ambient turbulence term is included and the overall eddy viscosity is given by Ainslie [23].

$$\varepsilon = FK_1 B_w (U_i - U_c) + \varepsilon_{amb} \quad (29)$$

Where the filter function  $F$  is a factor applied for near wake conditions. This filter can be introduced to allow for the build up of turbulence on wake mixing. The dimensionless constant  $K_1$  is a constant value over the whole flow field and a value of 0.015 is used.

The ambient eddy viscosity term is calculated by the following equation,

$$\varepsilon_{amb} = F.K_k^2 . I_{amb} / 100 \quad (30)$$

$K_k$  is the Von Karman constant with a value of 0.4. Due to comparisons between the model and measurements reported by Taylor [24], the filter function  $F$  is fixed at unity.

The centre line velocity deficit can be calculated at the start of the wake model ( two diameters downstream ) using the following empirical equation by Ainslie [25].

$$D_{mi} = 1 - \frac{U_c}{U_i} = C_t - 0.05 - [(16C_t - 0.5)I_{amb} / 1000] \quad (31)$$

Assuming a Gaussian wind speed profile and momentum conservation an expression for the relationship between the deficit  $D_m$  and the width parameter  $B_w$  is obtained as,

$$B_w = \sqrt{\frac{3.56C_t}{8D_m(1 - 0.5D_m)}} \quad (32)$$

Using the above equations, the average eddy viscosity at a distance 2D downstream of the turbine can be calculated. The equations can then be solved for the centre- line deficit and width parameter further downstream.

Assuming to the Gaussian profile, the velocity deficit a distance 'r' from the wake centerline is given by,

$$D_{m,r} = \exp[-3.56(r/B_w)^2] \quad (33)$$

Therefore the wake width W is given by

$$W = B_w \sqrt{\frac{0.5}{3.56}} \quad (34)$$

### (ii) Turbulence in the wake

Using the eddy viscosity model, it is also possible to calculate the additional turbulence caused by the wake. The added turbulence is calculated using an empirical characterization by Quarton and Ainslie [26].

This characterization enables the added turbulence in the wake to be define as a function of ambient turbulence  $I_{amb}$ , the turbine thrust coefficient  $C_t$ , the distance X downstream from the rotor plane and the length of the near wake,  $X_n$ .

To improve the prediction, the characterization was subsequently amended slightly by Hassan [27].

$$I_{add} = 5.7C_t^{0.7} I_{amb}^{0.68} (x/x_n)^{-0.96} \quad (35)$$

Here all turbulence intensities are expressed as percentages. Using the value of added turbulence and the incident ambient turbulence, the turbulence intensity  $I_{tot}$  at any turbine position in the wake can be calculated as,

$$I_{tot} = \sqrt{(I_{amb}^2 + I_{add}^2)} \quad (36)$$



The near wake length  $X_n$  is calculated according to Vermeulen [28] in term of the rotor  $R$  and the thrust coefficient  $C_t$  as

$$x_n = \frac{nr_0}{\left(\frac{dr}{dx}\right)} \quad (37)$$

Where ,  $r_0 = R\sqrt{\frac{m+1}{2}}$  ,  $m = \frac{1}{\sqrt{1-C_t}}$  ,  $n = \frac{\sqrt{0.214+0.144m}(1-\sqrt{0.134+0.124m})}{(1-\sqrt{0.214+0.144m})\sqrt{0.134+0.124m}}$

and the wake growth rate is given by:

$$\frac{dr}{dx} = \sqrt{\left(\left(\frac{dr}{dx}\right)_a\right)^2 + \left(\left(\frac{dr}{dx}\right)_m\right)^2 + \left(\left(\frac{dr}{dx}\right)_\lambda\right)^2} \quad (38)$$

Where,  $\left(\frac{dr}{dx}\right)_a = 2.5I_0 + 0.005$  is the growth rate contribution due to ambient turbulence.

$$\left(\frac{dr}{dx}\right)_m = \frac{(1-m)\sqrt{1.49+m}}{(1+m)9.76}$$

is the contribution due to shear-generated turbulence. And,

$$\left(\frac{dr}{dx}\right)_\lambda = 0.012B\lambda$$

is the contribution due to mechanical turbulence, where B is number of turbine

blades and  $\lambda$  is the tip speed ratio.

### 5. Modeling the wind turbine power

As an application, the generalized Fokker-Planck equation is used to assess the uncertainty in the power output of a variable-speed wind turbine [29]. The dynamics of the wind turbine is given by the angular momentum theorem,

$$J \frac{\partial \omega}{\partial t} = \frac{P_{drive} - P_{brake}}{\omega} \quad (39)$$

Where  $\omega$  is the rotor speed,  $J$  the moment of inertia,  $P_{drive}$  the aerodynamic power captured by the wind turbine and  $P_{brake}$  the braking power from the generator. The generator power output is related to the braking power by the simple relation

$$P_G = \eta P_{brake} \quad (40)$$

$\eta$  is a constant.

The aerodynamic power is given by the algebraic relation

$$P_{drive} = \frac{\pi}{2} \rho R^2 C_p(\lambda, \theta) V^3 \quad (41)$$

Where  $\rho$  is the air density,  $R$  the rotor radius,  $\theta$  the blade pitch angle.

The tip speed ratio (TSR)  $\lambda$  is the rotor tip speed divided by the oncoming wind speed and is given by

$$\lambda = R\omega/V \quad (42)$$

The power coefficient  $C_p$  is defined as the power from the wind turbine divided by the power available in the wind.

### 6. Conclusion

Wind turbine wake aerodynamics has been extensively studied both experimentally and analytically. Nevertheless, their knowledge is far from being satisfactory. Many of the numerical models proposed show an acceptable degree of agreement with the experiments with which they are compared.

The models which depend on the least simplifying assumptions are better suited in dealing with different configuration and in reproducing wake development in detail. Some aspects of individual wake modeling, such as full near wake representation, rotor tower interaction, dynamic inflow, convergence problems, influence of atmospheric stability and others are still issues of active research.

One of the most important difficulties that have not been treated satisfactorily is the choice of appropriate input parameters to define ambient unperturbed flow particularly in complicated terrains. Usually, a comparison with wind tunnel experiments is reasonably straightforward, but when field experiments are used for comparison there are many difficulties and effects like meandering, that have not yet been satisfactorily modeled.

Improved understanding of complex wind turbine aerodynamics formalized in accurate, robust models will constitute a powerful capability for analyzing and designing wind energy machines of the future.

## 7. References

- [1] Vermeer L.J., Sorensen J.N, Crespo A. "Wind turbine wake aerodynamics". Progress in Aerospace Sciences 39(2003):pp. 476-510.
- [2] Garrad Hassan and Partners. "BLADED for windows- Theory Manual, "A design tool for wind turbines performance and loading". September, 2001.
- [3] Lanchester F.W. "A contribution to the theory of propulsion and the screw propeller". Trans Inst Naval Archi.1915;57:98.
- [4] Glauert H. "Aerodynamic theory". Vol. 4. Berlin, Germany:Julius Springer: 1935. pp. 169–360 (Chapter Division L).
- [5] Froude R.E. "On the part played in propulsion by difference of fluid pressure". Trans Roy Inst Naval Arch 1889;30:390–405.
- [6] Wu T.Y. "Flow through a heavily loaded actuator disc".Schiffstechnik1962;9:134–8 .
- [7] Greenberg M.D, Powers S.R "Nonlinear actuator disc theory and flow field calculations, including non-uniform loading". NASA CR 1672, NASA, 1970.
- [8] Greenberg M.D. "Nonlinear actuator disc theory". Z Flugwissensch 1972;20(3):90–8.
- [9] Conway J. "Analytical solutions for the actuator disk with variable radial distribution of load". J Fluid Mech 1995;297:327–55.
- [10] Conway J. "Exact actuator disk solution for non-uniform heavy loading and slipstream contraction". J Fluid Mech 1998;365:235–67.
- [11] Madsen H.A. "The actuator cylinder a flow model for vertical axis wind turbines". PhD dissertation, Aalborg University Centre, 1982.
- [12] Peyret R, Taylor T.D. "Computational methods for fluid flows". Berlin: Springer; 1983.
- [13] Sorensen J.N, Myken A. "Unsteady actuator disc model for horizontal axis wind turbines". J Wind Eng Ind Aerodyn 1992;39:139–49
- [14] Madsen H.A. "A CFD analysis for the actuator disc flow compared with momentum theory results". In: Pedersen B,editor. Proceedings of the 10th IEA Symposium on the Aerodynamics of Wind Turbines, Department of Fluid Mechanics, Technical University of Denmark, 1996.p. 109–24.
- [15] Madsen H.A, Rasmussen F. "Measured airfoil characteristics of three blade segments on a 19m hawt rotor" .In McAnulty K,editor. Proceedings of the Third IEA symposium on the Aerodynamics of Wind Turbines, ETSU, Harewell, 1990.
- [16] Sorensen J.N, Shen W.Z, Munduate X. "Analysis of wake states by a full-field actuator disc model". Wind Energy 1998;1:73–88.
- [17] Madsen H.A, Rasmussen F. "The influence of energy conversion and induction from large blade deflections". In:Proceedings of the European Wind Energy Conference,James & James, 1999. pp. 138–41.
- [18] Mikkelsen R, Sorensen J.N, Shen W.Z. "Modelling and analysis of the flow field around a coned rotor. Wind" Energy 2001;4:121–35.
- [19] Hoerner S.F. "Fluid-dynamic drag. Hoerner Fluid Dynamics",BrickTown, N.J. USA, 1965.
- [20] Hansen M.O.L. "Polar for NACA 63-415 airfoil". Report ET-AFM-9902, Technical University of Denmark, Department of Energy Engineering, Lyngby, Denmark,1999.
- [21] Miller R.H. "The aerodynamic and dynamic analysis of horizontal axis wind turbines". J Wind Eng Ind Aerodyn 1983;15:329–40.

- [22] Prandtl L. "Bemerkungen zur Theorie der freien Turbulenz", ZAMM, 22(5), 1942.
- [23] Ainslie J.F, "Calculating the flow field in the wake of wind turbines", Journal of Wind Engineering and Industrial Aerodynamics, Vol 27, 1988.
- [24] Taylor G .J, "Wake Measurements on the Nibe Wind Turbines in Denmark", National Power, ETSU WN 5020, 1990.
- [25] Ainslie J.F, "Development of an Eddy Viscosity model of a Wind Turbine Wake", CERL Memorandum TPRD/L/AP/0081/M83, 1983.
- [26] Quarton D.C and Ainslie J.F, "Turbulence in Wind Turbine Wakes", J.Wind Eng, Vol. 14 No. 1, 1990.
- [27] Hassan U. "A Wind Tunnel Investigation of the Wake Structure within Small Wind Turbine Farms", Department of Energy, E/5A/CON/5113/1890, 1992.
- [28] Vermeulen P and Bultjes P, "Mathematical Modelling of Wake Interaction in Wind Turbine Arrays, Part 1", report TNO 81-01473, 1981.
- [29] Juliet B, Yannick P, Hana B, Gilles F "On the Fokker-Planck Equation for Stochastic Hybrid Systems: Application to a Wind Turbine Model". Power and Energy System Plateau de Moulon,France.

3/14/2009